

FAST TOEPLITZ EIGENVALUE COMPUTATIONS, JOINING INTERPOLATION-EXTRAPOLATION MATRIX-LESS ALGORITHMS AND SIMPLE-LOOP THEORY

M. Bogoya^{*1}, S.E. Ekström^{†2}, and S. Serra-Capizzano^{‡1}

¹University of Insubria, Como, Italy., Dipartimento di Scienza e Alta Tecnologia.

²Uppsala University, Uppsala, Sweden., Department of Information Technology, Division of Scientific Computing.

January 7, 2022

Abstract

Under appropriate technical assumptions, the simple-loop theory allows to deduce various types of asymptotic expansions for the eigenvalues of Toeplitz matrices generated by a function f . Independently and under the milder hypothesis that f is even and monotonic over $[0, \pi]$, matrix-less algorithms have been developed for the fast eigenvalue computation of large Toeplitz matrices, within a linear complexity in the matrix order: behind the high efficiency of such algorithms there are the expansions predicted by the simple-loop theory, combined with the extrapolation idea.

Here we focus our attention on a change of variable, followed by the asymptotic expansion of the new variable, and we adapt the matrix-less algorithm to the considered new setting.

Numerical experiments show a higher precision (till machine precision) and the same linear computation cost, when compared with the matrix-less procedures already presented in the relevant literature. Among the advantages, we concisely mention the following: a) when the coefficients of the simple-loop function are analytically known, the algorithm computes them perfectly; b) while the proposed algorithm is better or at worst comparable to the previous ones for computing the inner eigenvalues, it is extremely better for the computation of the extreme eigenvalues.

Keywords: Eigenvalue computation, Toeplitz matrix, Matrix-less method, Asymptotic expansion.

MSC Classes: Primary 15B05, 65F15, 65D05, 47B35. Secondary 15A18, 47A38.

1 INTRODUCTION

The target of this note is to design fast procedures for the computation of all the spectra of large Toeplitz matrices having an even generating function which is monotone in the interval $(-\pi, \pi)$. For the

*johanmanuel.bogoya@uninsubria.it

†sven-erik.ekstrom@it.uu.se

‡s.serracapizzano@uninsubria.it

formal definition of Toeplitz matrix generated by a Lebesgue integrable function over the basic interval $Q \equiv (-\pi, \pi)$ see the first lines of Section 2.

This topic has been studied in the recent years by several researchers. Indeed, taking into account a clear numerical evidence developed in a systematic series of the numerical tests, in [15] the second author formulated the following conjecture.

Conjecture 1.1. *Let l, g be two real-valued even functions with $g > 0$ on $(0, \pi)$, and suppose that $f \equiv \frac{l}{g}$ is monotone increasing over $(0, \pi)$. Set $X_n \equiv T_n^{-1}(g)T_n(l)$ for all n . Then, for every integer $\alpha \geq 0$, every n , and every $j = 1, \dots, n$, the following asymptotic expansion holds:*

$$\lambda_j(X_n) = f(\theta_{j,n}) + \sum_{k=1}^{\alpha-1} c_k(\theta_{j,n})h^k + E_{j,n,\alpha},$$

where:

- the eigenvalues of X_n are arranged in non-decreasing order, $\lambda_1(X_n) \leq \dots \leq \lambda_n(X_n)$;¹
- $\{c_k\}_{k=1}^{\infty}$ is a sequence of functions from $(0, \pi)$ to \mathbb{R} which depends only on l, g ;
- $h \equiv \frac{1}{n+1}$ and $\theta_{j,n} \equiv \frac{j\pi}{n+1} = j\pi h$;
- $E_{j,n,\alpha} = O(h^\alpha)$ is the remainder (the error), which satisfies the inequality $|E_{j,n,\alpha}| \leq \kappa_\alpha h^\alpha$ for some constant κ_α depending only on α, l, g .

In the case where $g = 1$ identically, Conjecture 1.1 was originally formulated and supported through numerical experiments in [15]. Then the algorithmic proposal was extended and refined in [1, 12, 13, 14]. When $g \equiv 1$ and l satisfies further technical additional assumptions, those of the simple-loop method, Conjecture 1.1 was formally proved by Bogoya, Böttcher, Grudsky, and Maximenko in a series of papers [5, 6, 9].

However, again in the case of $g \equiv 1$, the power of the simple-loop method has been not exploited completely, since in the case of a continuous generating function, the distribution results reported in Theorem 2.2 imply that $\lambda_j(T_n(f)) = f(s_{j,n})$ with $s_{j,n}$ belonging to $(0, \pi)$ and distributed as the identity function. However, more is known and indeed also in the independent variable θ there exists an asymptotic expansion regarding exactly the points $s_{j,n}$.

This note deals with the adaptation of the interpolation-extrapolation algorithms to the previous change of variable, joined with a trick at the end points introduced in [8].

The numerical results are extremely precise, even compared with the already good performances described in [1, 12, 13, 14, 15], since it is not difficult to reach machine precision, and the complexity is still linear.

The present note is organized as follows. Preliminary definitions, tools, and results are concisely reported in Section 2. Section 3 presents the new adapted algorithm for computing the Toeplitz eigenvalues: as in [14], our technique combines the extrapolation procedure proposed in [1, 15] – which allows the computation of *some* of the eigenvalues of X_n – with an appropriate interpolation process, designed for the simultaneous computation of *all* the eigenvalues of X_n , with the additional end point trick in [8]. In Section 4 we present the numerical experiments, while in Section 5 we draw conclusions and we list few open problems for research lines to be investigated in the next future.

¹Note that the eigenvalues of X_n are real, because $T_n(g)$ is symmetric positive definite and X_n is similar to the symmetric matrix $T_n^{-\frac{1}{2}}(g)T_n(l)T_n^{-\frac{1}{2}}(g)$.

2 PRELIMINARIES AND TOOLS

For a real or complex valued function f in $L^1[-\pi, \pi]$, let $\mathbf{a}_j(f)$ be its j th Fourier coefficient, i.e.

$$\mathbf{a}_j(f) \equiv \frac{1}{2\pi} \int_{-\pi}^{\pi} f(\theta) e^{-ij\theta} d\theta, \quad j \in \mathbb{Z},$$

and consider the sequence $\{T_n(f)\}_{n=1}^{\infty}$ of the $n \times n$ Toeplitz matrices defined by $T_n(f) \equiv (\mathbf{a}_{j-k}(f))_{j,k=0}^{n-1}$. The function f is customarily referred to as the generating function of this sequence.

As a second step, we introduce some notations and definitions concerning general sequences of matrices. For any function F defined on the complex field and for any matrix A_n of size d_n , by the symbol $\Sigma_\lambda(F, A_n)$, we denote the mean

$$\Sigma_\lambda(F, A_n) = \frac{1}{d_n} \sum_{j=1}^{d_n} F[\lambda_j(A_n)],$$

while by the symbol $\Sigma_\sigma(F, A_n)$, we denote the mean

$$\Sigma_\sigma(F, A_n) = \frac{1}{d_n} \sum_{j=1}^{d_n} F[\sigma_j(A_n)].$$

Definition 2.1. Given a sequence $\{A_n\}$ of matrices of size d_n with $d_n < d_{n+1}$ and given a Lebesgue-measurable function ψ defined over a measurable set $K \subset \mathbb{R}^\nu$, $\nu \in \mathbb{N}^+$, of finite and positive Lebesgue measure $\mu(K)$, we say that $\{A_n\}$ is distributed as (ψ, K) in the sense of the eigenvalues if for any continuous function F with bounded support, the following limit relation holds

$$\lim_{n \rightarrow \infty} \Sigma_\lambda(F, A_n) = \frac{1}{\mu(K)} \int_K F(\psi) d\mu.$$

In this case, we write in short $\{A_n\} \sim_\lambda (\psi, K)$. Furthermore we say that $\{A_n\}$ is distributed as (ψ, K) in the sense of the singular values if for any continuous function F with bounded support, the following limit relation holds

$$\lim_{n \rightarrow \infty} \Sigma_\sigma(F, A_n) = \frac{1}{\mu(K)} \int_K F(|\psi|) d\mu.$$

In this case, we write in short $\{A_n\} \sim_\sigma (\psi, K)$, which is equivalent to $\{A_n^* A_n\} \sim_\lambda (|\psi|^2, K)$.

In Remark 2.1 we provide an informal meaning of the notion of eigenvalue distribution. For the singular value distribution similar statements can be written.

Remark 2.1. *The informal meaning behind the above definition is the following. If ψ is continuous, n is large enough, and*

$$\left\{ \mathbf{x}_j^{(d_n)}, j = 1, \dots, d_n \right\}$$

is an equispaced grid on K , then a suitable ordering $\lambda_j(A_n)$, $j = 1, \dots, d_n$, of the eigenvalues of A_n is such that the pairs $\{(\mathbf{x}_j^{(d_n)}, \lambda_j(A_n))\}$, $j = 1, \dots, d_n$ reconstruct approximately the hypersurface

$$\{(\mathbf{x}, \psi(\mathbf{x})), \mathbf{x} \in K\}.$$

In other words, the spectrum of A_n ‘behaves’ like a uniform sampling of ψ over K . For instance, if $\nu = 1$, $d_n = n$, and $K = [a, b]$, then the eigenvalues of A_n are approximately equal to $\psi(a + \frac{j}{n}(b-a))$, $j = 1, \dots, n$, for n large enough and up to at most $o(n)$ outliers. Analogously, if we have $\nu = 2$, $d_n = n^2$, and $K = [a_1, b_1] \times [a_2, b_2]$, then the eigenvalues of the matrix A_n are approximately equal to $\psi(a_1 + \frac{j}{n}(b_1 - a_1), a_2 + \frac{k}{n}(b_2 - a_2))$, $j, k = 1, \dots, n$, for n large enough and up to at most $o(n^2)$ outliers.

The asymptotic distribution of eigenvalues and singular values of Toeplitz matrix sequences has been studied deeply and continuously in the last century (for example see [2, 3, 10, 16, 17] and references therein). The starting point of this theory, which contains many extensions and other results, is a famous theorem of Szegő [18], which we report in the version due to Tyrtysnikov and Zamarashkin [25].

Theorem 2.2. *If f is integrable over $Q \equiv (-\pi, \pi)$, and if $\{T_n(f)\}$ is the sequence of Toeplitz matrices generated by f , then*

$$\{T_n(f)\} \sim_\sigma (f, Q).$$

Moreover, if f is also real-valued, then each matrix $T_n(f)$ is Hermitian and

$$\{T_n(f)\} \sim_\lambda (f, Q).$$

Furthermore, strong localization results are known in the case where the generating function is real-valued, as stated in [20, Th.2.2] which we partly report below.

Theorem 2.3. *If f is integrable and real-valued almost everywhere over $Q \equiv (-\pi, \pi)$, m is the essential infimum of f , M is the essential supremum of f , and if $\{T_n(f)\}$ is the sequence of Toeplitz matrices generated by f , then*

$$\lambda_j(T_n(f)) \in (m, M)$$

for every $j = 1, \dots, n$, for every positive integer n , under the assumption that $m < M$. Moreover, if $m = M$ then the generating function f is constant almost everywhere and trivially we conclude that $T_n(f)$ coincides with m times the identity matrix.

2.1 THE SIMPLE-LOOP CASE

For $\alpha > 0$, the well-known weighted Wiener algebra W^α is the collection of all functions $f: \mathbb{T} \rightarrow \mathbb{C}$ whose Fourier coefficients satisfy

$$\|f\|_\alpha \equiv \sum_{j=-\infty}^{\infty} |\mathbf{a}_j(f)| (|j| + 1)^\alpha < \infty.$$

It is easy to see that if $f \in W^\alpha$ then $f \in C^{[\alpha]}[-\pi, \pi]$, hence the constant α is measuring the smoothness of the symbol f . In what follows we extend every symbol f to the whole real line in the natural way turning it into a 2π -periodic function, and we denote this extension by f as well.

The simple-loop class, denoted by SL^α , consists in the collection of all the real-valued symbols in W^α tracing out a simple-loop over the interval $[-\pi, \pi]$ with the following properties:

- (i) the range of f is a segment $[0, \mu]$ with $\mu > 0$;
- (ii) $f(0) = f(2\pi) = 0$, $f''(0) = f''(2\pi) > 0$;
- (iii) there is a unique $\theta_0 \in [0, 2\pi]$ such that $f(\theta_0) = \mu$, $f'(\theta) > 0$ for $\theta \in (0, \theta_0)$ and $f'(\theta) < 0$ for $\theta \in (\theta_0, 2\pi)$.

Note that if $f \in \text{SL}^\alpha$ then $f'(0) = f'(2\pi) = 0$, and that $\theta_0 = \pi$ for every even symbol, i.e. a symbol satisfying $f(\theta) = f(-\theta)$ for $\theta \in \mathbb{R}$.

Consider an even symbol $f \in \text{SL}^\alpha$ with $\alpha > 2$. For a $n \times n$ matrix A let $\lambda_j(A)$ ($j = 1, \dots, n$) be its eigenvalues. In the works [5, 6, 7, 8], for example, the authors state that

(i) the eigenvalues of $T_n(f)$ are all distinct, i.e.

$$\lambda_1(T_n(f)) < \lambda_2(T_n(f)) < \cdots < \lambda_n(T_n(f));$$

(ii) the numbers $s_{j,n} \equiv [f|_{[0,\pi]}]^{-1}(\lambda_j(T_n(f)))$ ($j = 1, \dots, n$) satisfy

$$(n+1)s_{j,n} + \eta(s_{j,n}) = \pi j + E_{j,n,\alpha}, \quad (2.1)$$

where $E_{j,n,\alpha}$ is an error term satisfying certain bounding condition, and η is a function depending only on f with certain smoothness depending on α .

(iii) the previous equation (2.1) has exactly one solution $s_{j,n} \in [0, \pi]$ for each $j = 1, \dots, n$.

In the bulk of the so-called *simple-loop method*, the authors use the Banach fixed-point theorem to iterate over (2.1) and solve it for $s_{j,n}$, obtaining an expansion of the kind (see [5, Th.2.2] for example)

$$\lambda_j(T_n(f)) = f(s_{j,n}), \quad s_{j,n} = \theta_{j,n} + \sum_{k=1}^{\lfloor \alpha \rfloor} r_k(\theta_{j,n})h^k + E_{j,n,\alpha}, \quad (2.2)$$

where

- the numbers $s_{j,n}$ are arranged in nondecreasing order;
- $h \equiv \frac{1}{n+1}$ and $\theta_{j,n} \equiv \pi j h$;
- the coefficients r_k depend only on f and can be found explicitly, for example

$$\begin{aligned} r_1 &= -\eta, & r_3 &= -\eta(\eta')^2 - \frac{1}{2}\eta^2\eta'', \\ r_2 &= \eta\eta', & r_4 &= \eta(\eta')^3 + \frac{3}{2}\eta^2\eta'\eta'' + \frac{1}{6}\eta^3\eta'''. \end{aligned}$$

- $E_{j,n,\alpha} = O(h^\alpha)$ is the remainder (error) term, which satisfies the bounding $|E_{j,n,\alpha}| \leq \kappa_\alpha h^\alpha$ for some constant κ_α depending only on α and f .

Using the expansion (2.2) and the smoothness of the symbol f , the authors apply f to both sides obtaining an expansion of the kind

$$\lambda_j(T_n(f)) = f(\theta_{j,n}) + \sum_{k=1}^{\lfloor \alpha \rfloor} c_k(\theta_{j,n})h^k + E_{j,n,\alpha}, \quad (2.3)$$

with similar characteristics but where the coefficients c_k involve the symbol and its derivatives, for instance $c_1 = -f'\eta$ and $c_2 = f'\eta\eta' + \frac{1}{2}f''\eta^2$. The previous works [8, 13, 14, 15] used (2.3) as the basic expansion. We noticed that (2.3) is absorbing all the almost non-increasing consequences of f at $\{0, \pi\}$ and all the related troubles that the derivatives of f can produce. Hence, we decided to work with (2.2) instead.

Indeed, in the light of Theorem 2.2, since f is even and real-valued, we find $\{T_n(f)\} \sim_\lambda (f, [0, \pi])$. Consequently we deduce

$$\{\text{diag}_{j=1,\dots,n}(s_{j,n})\} \sim_\lambda (\text{id}, [0, \pi]), \quad \text{id}(\theta) \equiv \theta,$$

with $s_{j,n} \in (0, \pi)$, by virtue of Theorem 2.3. Notice that the function $\text{id}(\cdot)$ is very basic, and, as already claimed, when compared with the study and the proposals in [5, 6, 9, 8, 12, 13, 14, 15], the troubles that the derivatives of f produce are completely removed: these nice features are clearly evident by looking at the high precision of the numerical computations, reported in Section 4, containing the numerical experiments.

3 THE ALGORITHM

Our algorithm is based on the expansion (2.2) and is an evolution of the algorithms proposed in [8, 13, 14, 15]. As in the mentioned works it is suited for parallel implementation and can be called matrix-less since it does not require to calculate or even, to store the matrix entries. For every $n \in \mathbb{N}$ let $h \equiv \frac{1}{n+1}$ and $\theta_{j,n} \equiv \pi j h$, thus the collection $\{\theta_{j,n}\}_{j=0}^{n+1}$ is a regular grid for the interval $[0, \pi]$ with step size πh . We will use similar notations for n and h , for example, h_k means $\frac{1}{n_k+1}$, and so on. We assume that

- the symbol f is even and real-valued, strictly increasing in the interval $[0, \pi]$, and $f(0) = 0$;
- n_1 and α are fixed natural numbers and $n \gg n_1$;
- for $k = 1, \dots, \alpha$ let $n_k \equiv 2^{k-1}(n_1 + 1) - 1$;
- for $j_1 = 1, \dots, n_1$ and $k = 1, \dots, \alpha$, let $j_k \equiv 2^{k-1}j_1$.

Note that j_k depends on j_1 , and similarly, n_k depends on n_1 , but for notation simplicity, we suppressed those dependencies. The indexes j_k and the matrix sizes n_k were calculated in such a way that

$$\theta_{j_1, n_1} = \theta_{j_2, n_2} = \dots = \theta_{j_\alpha, n_\alpha},$$

which is the key idea of the following extrapolation phase, see Figure 1. We also want to emphasize that f is not necessarily simple-loop.

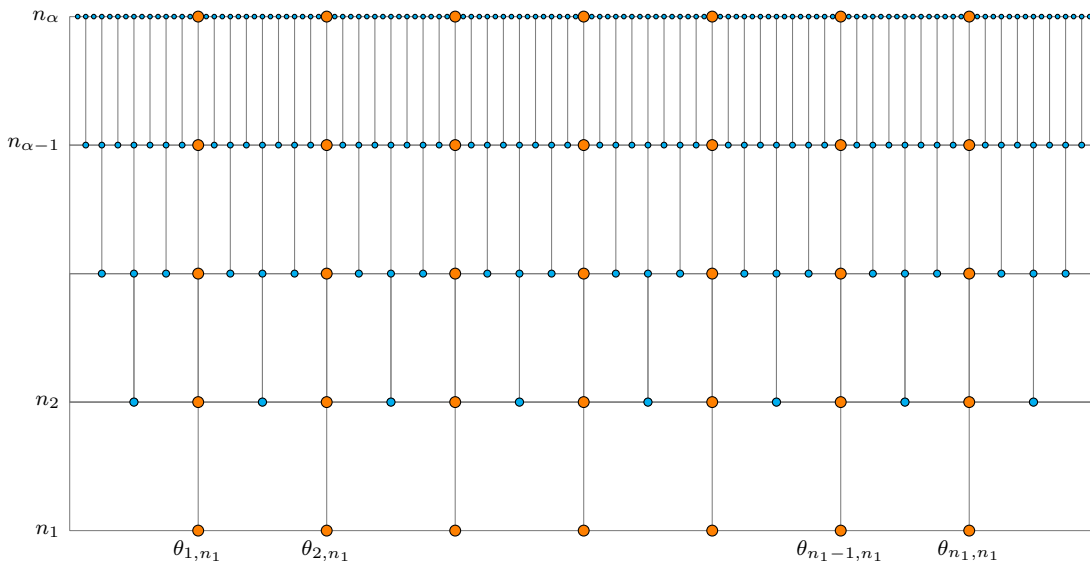


Figure 1: The regular grids $\{\theta_{j,n_k}\}$ for $j = 1, \dots, n_k$ and $k = 1, \dots, \alpha$. In the precomputing phase we will need to calculate the eigenvalues of $T_{n_k}(f)$ for $k = 1, \dots, \alpha$ corresponding to the blue and orange dots combined, but in the interpolation phase, we will use only the eigenvalues corresponding to the orange dots, that is $\lambda_{j_k}(T_{n_k}(f))$ for $j_1 = 1, \dots, n_1$ and $k = 1, \dots, \alpha$.

As in [8, 13, 14, 15], our algorithm is designed to calculate eigenvalues for “big” matrix sizes n with respect to n_1, \dots, n_α , meaning that, from a computational viewpoint, the calculation of the eigenvalues of $T_n(f)$ is hard while for $T_{n_k}(f)$ can be easily done with any standard eigensolver (i.e. **Eigenvalues** in MATHEMATICA or **eig** in MATLAB). But our proposal is able to reach machine precision accuracy easily.

The algorithm has two phases, the first one involves an extrapolation procedure, and the second one consists in a local interpolation technique. As a precomputing phase we need to calculate the eigenvalues of $T_n(f)$ for $n = n_1, \dots, n_\alpha$.

Extrapolation For each fixed $j_1 = 1, \dots, n_1$ let $\sigma_{j_1} \equiv \theta_{j_1, n_1} = \dots = \theta_{j_\alpha, n_\alpha}$ (see the orange dots in Figure 1), and apply α times the expansion (2.2) obtaining

$$\begin{aligned} \lambda_{j_1}(T_{n_1}(f)) - f(\sigma_{j_1}) &= r_1(\sigma_{j_1})h_1 + r_2(\sigma_{j_1})h_1^2 + \dots + r_\alpha(\sigma_{j_1})h_1^\alpha + E_{j_1, n_1, \alpha}, \\ \lambda_{j_2}(T_{n_2}(f)) - f(\sigma_{j_1}) &= r_1(\sigma_{j_1})h_2 + r_2(\sigma_{j_1})h_2^2 + \dots + r_\alpha(\sigma_{j_1})h_2^\alpha + E_{j_2, n_2, \alpha}, \\ &\vdots \\ \lambda_{j_\alpha}(T_{n_\alpha}(f)) - f(\sigma_{j_1}) &= r_1(\sigma_{j_1})h_\alpha + r_2(\sigma_{j_1})h_\alpha^2 + \dots + r_\alpha(\sigma_{j_1})h_\alpha^\alpha + E_{j_\alpha, n_\alpha, \alpha}. \end{aligned}$$

Let $\hat{r}_k(\sigma_{j_1})$ be the approximation of $r_k(\sigma_{j_1})$ obtained by removing all the error terms $E_{j_k, n_k, \alpha}$ and solving the resulting linear system:

$$\begin{bmatrix} h_1 & h_1^2 & \dots & h_1^\alpha \\ h_2 & h_2^2 & \dots & h_2^\alpha \\ \vdots & \vdots & \ddots & \vdots \\ h_\alpha & h_\alpha^2 & \dots & h_\alpha^\alpha \end{bmatrix} \begin{bmatrix} \hat{r}_1(\sigma_{j_1}) \\ \hat{r}_2(\sigma_{j_1}) \\ \vdots \\ \hat{r}_\alpha(\sigma_{j_1}) \end{bmatrix} = \begin{bmatrix} \lambda_{j_1}(T_{n_1}(f)) \\ \lambda_{j_2}(T_{n_2}(f)) \\ \vdots \\ \lambda_{j_\alpha}(T_{n_\alpha}(f)) \end{bmatrix} - f(\sigma_{j_1}) \begin{bmatrix} 1 \\ 1 \\ \vdots \\ 1 \end{bmatrix}. \quad (3.1)$$

As mentioned in previous works, a variant of this extrapolation strategy was first suggested by Albrecht Böttcher in [5, §7] and is analogous to the Richardson extrapolation employed in the context of Romberg integration [22, §3.4].

Interpolation For any $j \in \{1, \dots, n\}$ we will estimate $r_k(\theta_{j, n})$. If $\theta_{j, n}$ coincides with one of the points in the grid $\{\theta_{0, n_1}, \dots, \theta_{n_1+1, n_1}\}$, then we have the approximations $\hat{r}(\theta_{j, n})$ from the extrapolation phase for free. In any other case, we will do it by interpolating the data

$$(\theta_{0, n_k}, \hat{r}_k(\theta_{0, n_k})), (\theta_{1, n_k}, \hat{r}_k(\theta_{1, n_k})), \dots, (\theta_{n_k+1, n_k}, \hat{r}_k(\theta_{n_k+1, n_k})),$$

for $k = 1, \dots, \alpha$, and then evaluating the resulting polynomial at $\theta_{j, n}$. This interpolation can be done in many ways, but to avoid spurious oscillations explained by the Runge phenomenon [11, p.78], and following the strategy of the previous works, we decided to do it considering only the $\alpha - k + 5$ points in the grid $\{\theta_{0, n_1}, \dots, \theta_{n_1+1, n_1}\}$ which are closest to $\theta_{j, n}$. Those points can be determined uniquely unless $\theta_{j, n}$ is the mid point of two consecutive points in the grid, in which case we can take any of the possible two choices.

Finally, our eigenvalue approximation with k terms, is given by

$$\hat{\lambda}_{j, k}^{\text{NAS}}(T_n(f)) \equiv f\left(\theta_{j, n} + \sum_{\ell=0}^{k-1} \hat{r}_\ell(\theta_{j, n})h^\ell\right), \quad (3.2)$$

where $k = 1, \dots, \alpha$, and NAS stands for ‘‘Numerical Algorithm in the variable $s_{j, k}$ ’’.

Remark 3.1. *To get the best results possible, in the precomputing phase, we advise to use the proposed algorithm (3.2), calculating the eigenvalues of $T_n(f)$ for $n = n_1, \dots, n_\alpha$ with a significant number of precision digits, let’s say 60. For $\alpha = 5$ and $n_1 = 100$, for instance, this can be done in a standard computer in a few minutes, and it only needs to be done once. While for the extrapolation phase (3.1), we advice to do it with the largest α possible.*

4 NUMERICAL EXPERIMENTS

Let $\lambda_{j,k}^{\text{SL}}(T_n(f))$ be the k th term approximation of $\lambda_j(T_n(f))$ obtained with the simple-loop method in the variable $s_{j,n}$, that is

$$\lambda_{j,k}^{\text{SL}}(T_n(f)) \equiv f\left(\theta_{j,n} + \sum_{k=1}^{k-1} r_k(\theta_{j,n})h^k\right),$$

where $\theta_{j,n} = \pi j h$. Let also $\lambda_{j,k}^{\text{NA}}(T_n(f))$ be the k th term approximation of $\lambda_j(T_n(f))$ given by the Numerical Algorithm in [14] and finally, let $\lambda_{j,k}^{\text{MNA}}(T_n(f))$ be the respective approximation given by the Modified Numerical Algorithm [8, §4]. In order to compare the results of the different methods we use the following notation for the absolute individual errors

$$\begin{aligned} \varepsilon_{j,n,k}^{\text{SL}} &\equiv |\lambda_j(T_n(f)) - \lambda_{j,k}^{\text{SL}}(T_n(f))|, & \varepsilon_{j,n,k}^{\text{NA}} &\equiv |\lambda_j(T_n(f)) - \lambda_{j,k}^{\text{NA}}(T_n(f))|, \\ \varepsilon_{j,n,k}^{\text{MNA}} &\equiv |\lambda_j(T_n(f)) - \lambda_{j,k}^{\text{MNA}}(T_n(f))|, & \varepsilon_{j,n,k}^{\text{NAS}} &\equiv |\lambda_j(T_n(f)) - \lambda_{j,k}^{\text{NAS}}(T_n(f))|, \end{aligned}$$

and the respective maximum absolute errors

$$\begin{aligned} \varepsilon_{n,k}^{\text{SL}} &\equiv \max\{\varepsilon_{j,n,k}^{\text{SL}} : j = 1, \dots, n\}, & \varepsilon_{n,k}^{\text{NA}} &\equiv \max\{\varepsilon_{j,n,k}^{\text{NA}} : j = 1, \dots, n\}, \\ \varepsilon_{n,k}^{\text{MNA}} &\equiv \max\{\varepsilon_{j,n,k}^{\text{MNA}} : j = 1, \dots, n\}, & \varepsilon_{n,k}^{\text{NAS}} &\equiv \max\{\varepsilon_{j,n,k}^{\text{NAS}} : j = 1, \dots, n\}. \end{aligned}$$

We start with an example involving a well-known simple-loop symbol for which we can exactly calculate the coefficients r_k in (2.2) easily, thus we will be able to compare the accuracy of the different eigenvalue approximations.

Example 4.1 (A simple-loop symbol). Consider the even simple-loop symbol given by

$$f(\theta) := \frac{(1+\rho)^2}{2} \cdot \frac{1 - \cos(\theta)}{1 - 2\rho \cos(\theta) + \rho^2} \quad (0 \leq \theta \leq 2\pi), \quad (4.1)$$

for a constant $0 < \rho < 1$, see Figure 2. This symbol was inspired in the Kac–Murdock–Szegő Toeplitz matrices introduced in [19] and subsequently studied in [23, 24], which usually are present in important physics models. The respective Fourier coefficients can be explicitly calculated as $\mathbf{a}_k(f) = \frac{1}{4}(\rho^2 - 1)\rho^{|k|-1}$ for $k \neq 0$ and $\frac{1}{2}(1 + \rho)$ for $k = 0$. We then have

$$\|f\|_\alpha = \frac{1+\rho}{2} + \frac{\rho^2-1}{2\rho} \sum_{k=1}^{\infty} \rho^k (k+1)^\alpha,$$

which is finite for every $\alpha > 0$, the remaining simple-loop conditions are easily verified in Figure 2. Then $f \in \text{SL}^\alpha$ for any $\alpha > 0$. According to [8, §4], the function η in (2.1) is nicely given by

$$\eta(s) = 2 \arctan\left(\frac{\rho \sin(s)}{1 - \rho \cos(s)}\right).$$

The Figure 3 and the Table 1 shows that, in this case, the approximation $\lambda_{j,k}^{\text{MNA}}(T_n(f))$ can produce good results until the level $k = 2$ but it becomes unstable from this point on. While our algorithm (3.2) is still producing fine results in the 4th level and, for a matrix of size 4096, it reaches machine-precision from level 3. The Figure 3 reveals also, that for the symbol (4.1), our proposed algorithm (3.2) can match the exact asymptotic simple-loop expansion until level 4.

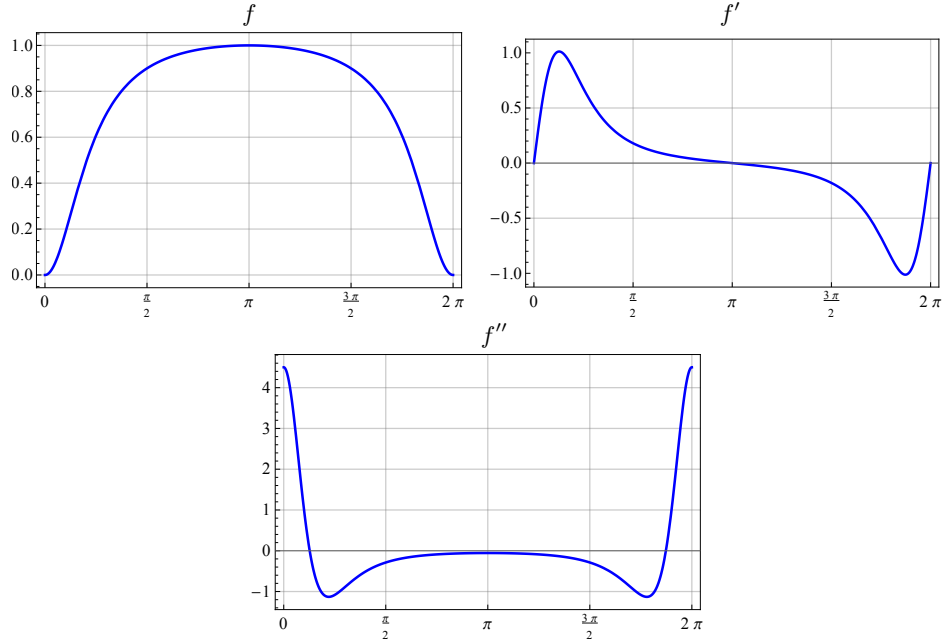


Figure 2: The symbol f in (4.1) and its first two derivatives for $\rho = \frac{1}{2}$.

n	256	512	1024	2048	4096
$\varepsilon_{n,1}^{\text{MNA}}$	3.0897×10^{-3}	1.5494×10^{-3}	7.7577×10^{-4}	3.8816×10^{-4}	1.9415×10^{-3}
$\varepsilon_{n,1}^{\text{NAS}}$	3.0897×10^{-3}	1.5494×10^{-3}	7.7577×10^{-4}	3.8816×10^{-4}	1.9415×10^{-4}
$(n+1)\varepsilon_{n,1}^{\text{NAS}}$	7.9405×10^{-1}	7.9482×10^{-1}	7.9517×10^{-1}	7.9534×10^{-1}	7.9542×10^{-1}
$\varepsilon_{n,2}^{\text{MNA}}$	1.5098×10^{-5}	3.7949×10^{-6}	9.5024×10^{-7}	2.3819×10^{-7}	5.9529×10^{-8}
$\varepsilon_{n,2}^{\text{NAS}}$	1.3575×10^{-5}	3.4113×10^{-5}	8.5515×10^{-7}	2.1407×10^{-7}	5.3553×10^{-8}
$(n+1)^2 \varepsilon_{n,2}^{\text{NAS}}$	8.9661×10^{-1}	8.9775×10^{-1}	8.9844×10^{-1}	8.9875×10^{-1}	8.9890×10^{-1}
$\varepsilon_{n,3}^{\text{MNA}}$	8.8167×10^{-8}	1.4780×10^{-8}	4.7324×10^{-9}	2.4238×10^{-9}	1.2270×10^{-9}
$\varepsilon_{n,3}^{\text{NAS}}$	5.4356×10^{-8}	6.8619×10^{-9}	8.6153×10^{-10}	1.0794×10^{-10}	1.3507×10^{-11}
$(n+1)^3 \varepsilon_{n,3}^{\text{NAS}}$	9.2267×10^{-1}	9.2640×10^{-1}	9.2778×10^{-1}	9.2852×10^{-1}	9.2887×10^{-1}
$\varepsilon_{n,4}^{\text{MNA}}$	6.6888×10^{-9}	3.1948×10^{-9}	1.5778×10^{-9}	7.8461×10^{-10}	3.8983×10^{-10}
$\varepsilon_{n,4}^{\text{NAS}}$	3.4700×10^{-10}	2.1887×10^{-11}	1.3740×10^{-12}	8.6077×10^{-14}	5.4131×10^{-15}
$(n+1)^4 \varepsilon_{n,4}^{\text{NAS}}$	1.5138×10^0	1.5158×10^0	1.5166×10^0	1.5172×10^0	1.5252×10^0

Table 1: The maximum errors $\varepsilon_{n,k}^{\text{MNA}}$, $\varepsilon_{n,k}^{\text{NAS}}$, and maximum normalized errors $(n+1)^k \varepsilon_{n,k}^{\text{NAS}}$ for the levels $k = 1, 2, 3, 4$ and different matrix sizes n , corresponding to the symbol (4.1) with $\rho = \frac{1}{2}$. We used a grid of size $n_1 = 100$.

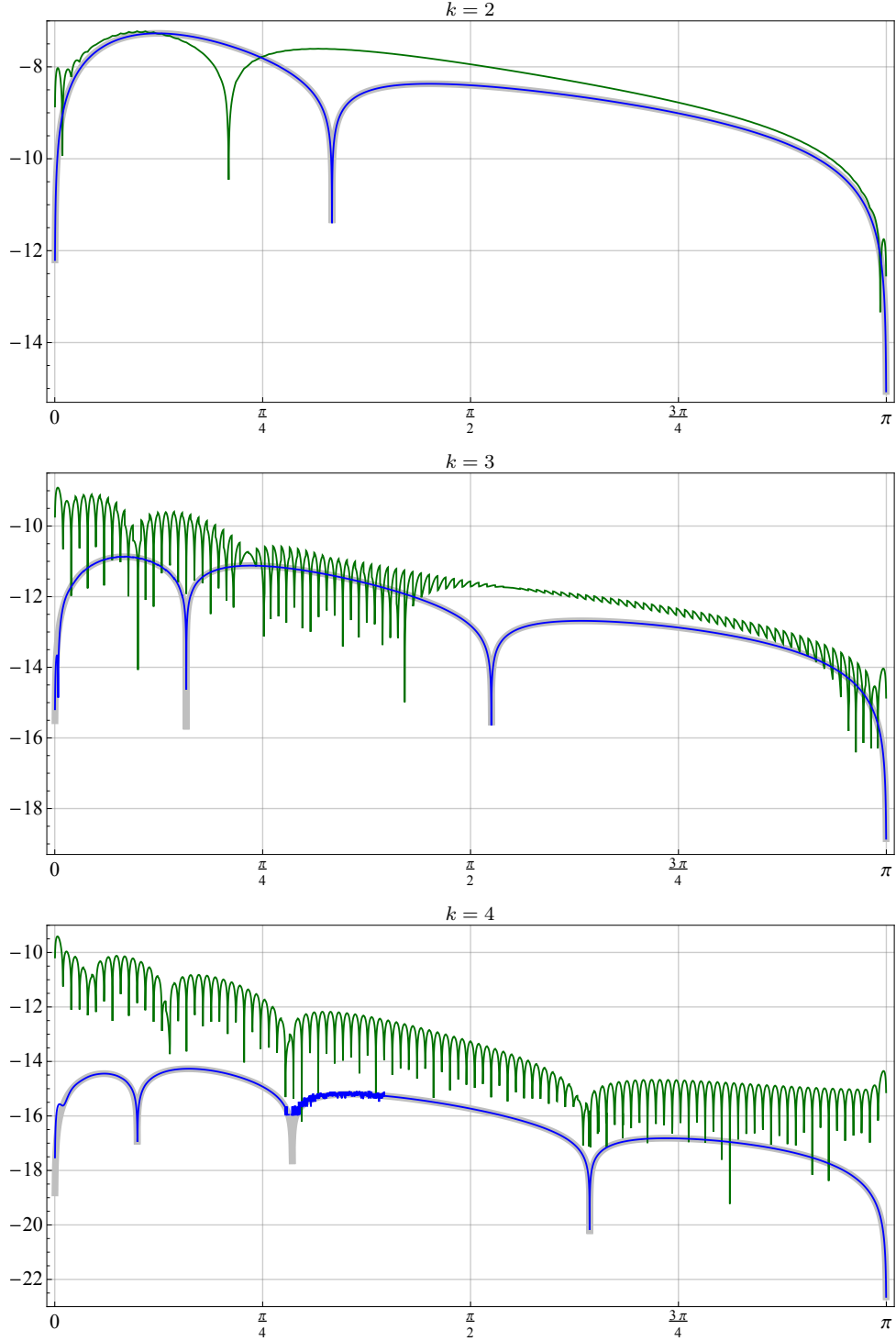


Figure 3: The base-10 logarithm for the individual errors $\varepsilon_{j,n,k}^{\text{SL}}$ (thick gray), $\varepsilon_{j,n,k}^{\text{MNA}}$ (green), and $\varepsilon_{j,n,k}^{\text{NAS}}$ (blue) for the symbol f in (4.1) with $\rho = \frac{1}{2}$, a matrix size $n = 4096$, a grid size $n_1 = 100$, and different levels k . The proposed numerical algorithm (3.2) is represented by the blue curve, while the exact asymptotic simple-loop expansion, by the gray curve.

Example 4.2 (A non-simple-loop symbol). We now test our algorithm with a Real Cosine Trigonometric Polynomial (RCTP), see [15, §1]. For $\ell \in \mathbb{Z}_+$, consider the symbol

$$f_\ell(\theta) \equiv (2 - 2 \cos(\theta))^\ell, \quad \theta \in Q. \quad (4.2)$$

The respective Fourier coefficients can be exactly calculated as $\mathbf{a}_k(f_\ell) = (-1)^k \binom{2\ell}{\ell+k}$ for $|k| \leq \ell$ and $\mathbf{a}_k(f_\ell) = 0$ in any other case, then the respective Toeplitz matrices $T_n(f_\ell)$ are banded with a band of size $2\ell + 1$. The case $\ell = 2$ was carefully studied by Barrera and Grudsky in [4], where they formally deduced that

$$s_{j,n} = \frac{\pi(j+1)}{n+2} + \frac{u_{1,j}}{n+2} + \frac{u_{2,j}}{(n+2)^2} + O(h^3),$$

with some bounded and continuous coefficients $u_{1,j}, u_{2,j}$. See Theorem 2.5 there. The previous expansion is slightly different from (2.2) but we were able to show that our algorithm is producing fine results in this case.

It is clear that $f_\ell \in W^\alpha$ for any $\ell \in \mathbb{Z}_+$ and any $\alpha > 0$, but f_ℓ is simple-loop only when $\ell = 1$ because $f_\ell''(0) = 0$ for $\ell \neq 1$. The Figures 5, 6, and the Tables 2, 3, show the data for the cases $\ell = 2, 3$. Since our method is based on the simple-loop expansion (2.2), we expected difficulties for the very first eigenvalues, corresponding to the point $\theta = 0$, nevertheless, the numerical approximations are good enough for machine precision purposes.

The Figure 4 shows a comparison between the individual errors $\varepsilon_{j,n,k}^{\text{NA}}$, given by the eigenvalue approximation of the numerical algorithm [15], and $\varepsilon_{j,n,k}^{\text{MNA}}$, which corresponds to its boundary modification given by [8, §4]. Then it is clear that the modified version works better.

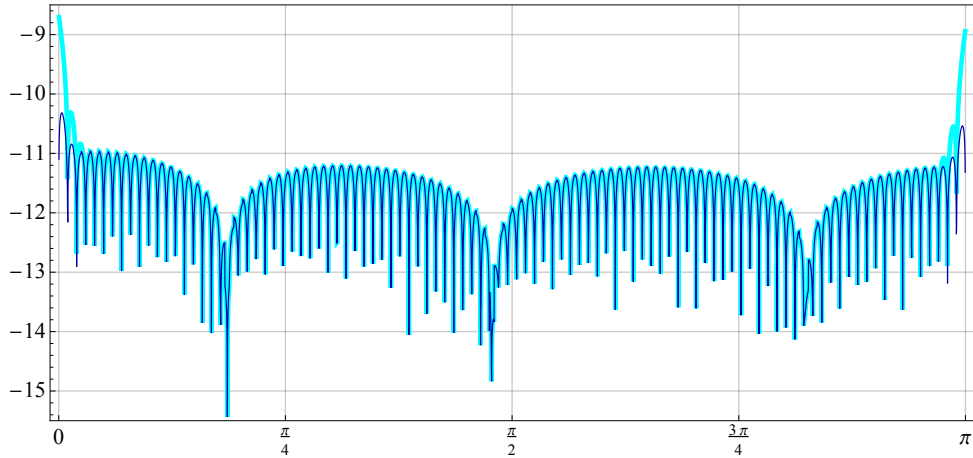


Figure 4: The base-10 logarithm for the individual errors $\varepsilon_{j,n,k}^{\text{NA}}$ (thick cyan curve) and $\varepsilon_{j,n,k}^{\text{MNA}}$ (thin blue curve), corresponding to the algorithms [15] and [8, §4], respectively. We worked with the symbol (4.2) where $\ell = 3$, level $k = 4$, a matrix size $n = 4096$, and a grid size $n_1 = 100$.

n	256	512	1024	2048	4096
$\varepsilon_{n,1}^{\text{MNA}}$	1.6269×10^{-2}	8.1578×10^{-3}	4.0848×10^{-3}	2.0439×10^{-3}	1.0223×10^{-3}
$\varepsilon_{n,1}^{\text{NAS}}$	1.6269×10^{-2}	8.1578×10^{-3}	4.0848×10^{-3}	2.0439×10^{-3}	1.0223×10^{-3}
$(n+1)\varepsilon_{n,1}^{\text{NAS}}$	4.1811×10^0	4.1850×10^0	4.1869×10^0	4.1878×10^0	4.1883×10^0
$\varepsilon_{n,2}^{\text{MNA}}$	2.2934×10^{-5}	5.7602×10^{-6}	1.4434×10^{-6}	3.6126×10^{-7}	9.0367×10^{-8}
$\varepsilon_{n,2}^{\text{NAS}}$	2.7270×10^{-5}	6.8421×10^{-6}	1.7136×10^{-6}	4.2880×10^{-7}	1.0725×10^{-7}
$(n+1)^2\varepsilon_{n,2}^{\text{NAS}}$	1.8011×10^0	1.8006×10^0	1.8004×10^0	1.8003×10^0	1.8002×10^0
$\varepsilon_{n,3}^{\text{MNA}}$	7.5158×10^{-8}	9.4903×10^{-9}	1.2050×10^{-9}	1.5758×10^{-10}	2.5206×10^{-11}
$\varepsilon_{n,3}^{\text{NAS}}$	6.9024×10^{-8}	8.6696×10^{-9}	1.0863×10^{-9}	1.3595×10^{-10}	1.7004×10^{-11}
$(n+1)^3\varepsilon_{n,3}^{\text{NAS}}$	1.1717×10^0	1.1704×10^0	1.1698×10^0	1.1695×10^0	1.1694×10^0
$\varepsilon_{n,4}^{\text{MNA}}$	3.7838×10^{-9}	2.2540×10^{-10}	1.6954×10^{-11}	5.9426×10^{-12}	3.2321×10^{-12}
$\varepsilon_{n,4}^{\text{NAS}}$	2.7800×10^{-9}	1.3631×10^{-10}	7.4328×10^{-12}	4.5503×10^{-13}	5.4968×10^{-14}
$(n+1)^4\varepsilon_{n,4}^{\text{NAS}}$	1.2128×10^1	9.4408×10^0	8.2044×10^0	8.2044×10^0	1.5487×10^1

Table 2: The maximum errors $\varepsilon_{n,k}^{\text{MNA}}$, $\varepsilon_{n,k}^{\text{NAS}}$, and maximum normalized errors $(n+1)^k\varepsilon_{n,k}^{\text{NAS}}$ for the levels $k = 1, 2, 3, 4$ and different matrix sizes n , corresponding to the symbol (4.2) with $\ell = 2$. We used a grid of size $n_1 = 100$.

n	256	512	1024	2048	4096
$\varepsilon_{n,1}^{\text{MNA}}$	9.1868×10^{-2}	4.6172×10^{-2}	2.3146×10^{-2}	1.1588×10^{-2}	5.7978×10^{-3}
$\varepsilon_{n,1}^{\text{NAS}}$	9.1868×10^{-2}	4.6172×10^{-2}	2.3146×10^{-2}	1.1588×10^{-2}	5.7978×10^{-3}
$(n+1)\varepsilon_{n,1}^{\text{NAS}}$	2.3610×10^1	2.3686×10^1	2.3725×10^1	2.3744×10^1	2.3753×10^1
$\varepsilon_{n,2}^{\text{MNA}}$	2.2588×10^{-4}	5.6759×10^{-5}	1.4227×10^{-5}	3.5615×10^{-6}	8.9091×10^{-7}
$\varepsilon_{n,2}^{\text{NAS}}$	3.0497×10^{-4}	7.6550×10^{-5}	1.9176×10^{-5}	4.7989×10^{-6}	1.2003×10^{-6}
$(n+1)^2\varepsilon_{n,2}^{\text{NAS}}$	2.0143×10^1	2.0146×10^1	2.0147×10^1	2.0148×10^1	2.0148×10^1
$\varepsilon_{n,3}^{\text{MNA}}$	9.5995×10^{-7}	1.2158×10^{-7}	1.5664×10^{-8}	2.1683×10^{-9}	3.7673×10^{-10}
$\varepsilon_{n,3}^{\text{NAS}}$	1.3355×10^{-6}	1.6765×10^{-7}	2.1002×10^{-8}	2.6281×10^{-9}	3.2868×10^{-10}
$(n+1)^3\varepsilon_{n,3}^{\text{NAS}}$	2.2669×10^1	2.2634×10^1	2.2617×10^1	2.2608×10^1	2.2604×10^1
$\varepsilon_{n,4}^{\text{MNA}}$	5.7200×10^{-9}	3.9578×10^{-10}	1.7663×10^{-10}	9.3710×10^{-11}	4.8060×10^{-11}
$\varepsilon_{n,4}^{\text{NAS}}$	7.6467×10^{-9}	4.8020×10^{-10}	3.0083×10^{-11}	1.8824×10^{-12}	1.1772×10^{-13}
$(n+1)^4\varepsilon_{n,4}^{\text{NAS}}$	3.3358×10^1	3.3258×10^1	3.3206×10^1	3.3181×10^1	3.3168×10^1

Table 3: The same as Table 2 but this time with $\ell = 3$.

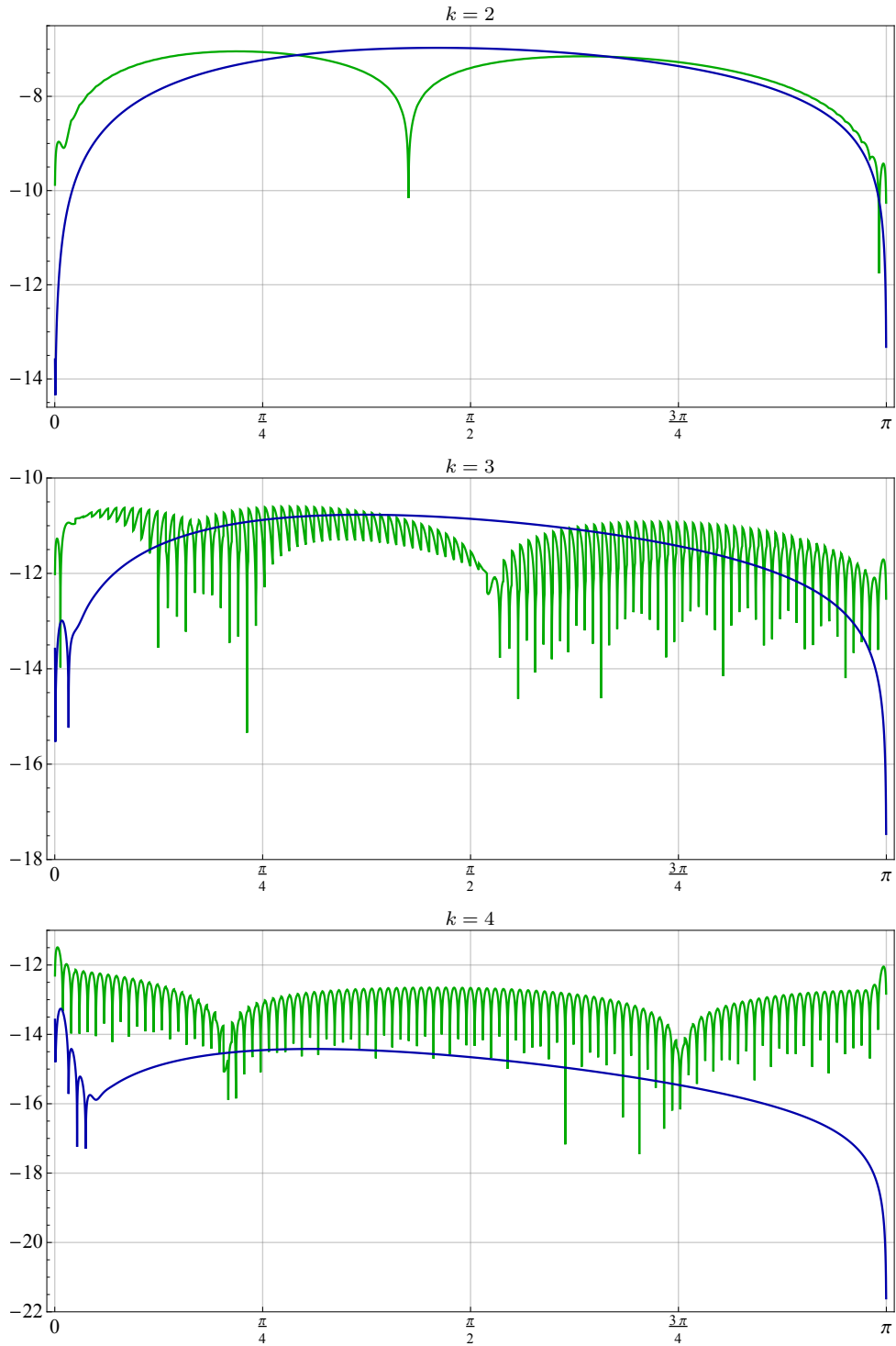


Figure 5: The base-10 logarithm for the individual errors $\varepsilon_{j,n,k}^{\text{SL}}$ (thick gray), $\varepsilon_{j,n,k}^{\text{MNA}}$ (green), and $\varepsilon_{j,n,k}^{\text{NAS}}$ (blue) for the RCTP symbol f_ℓ in (4.2) with $\ell = 2$, a matrix size $n = 4096$, a grid size $n_1 = 100$, and different levels k .

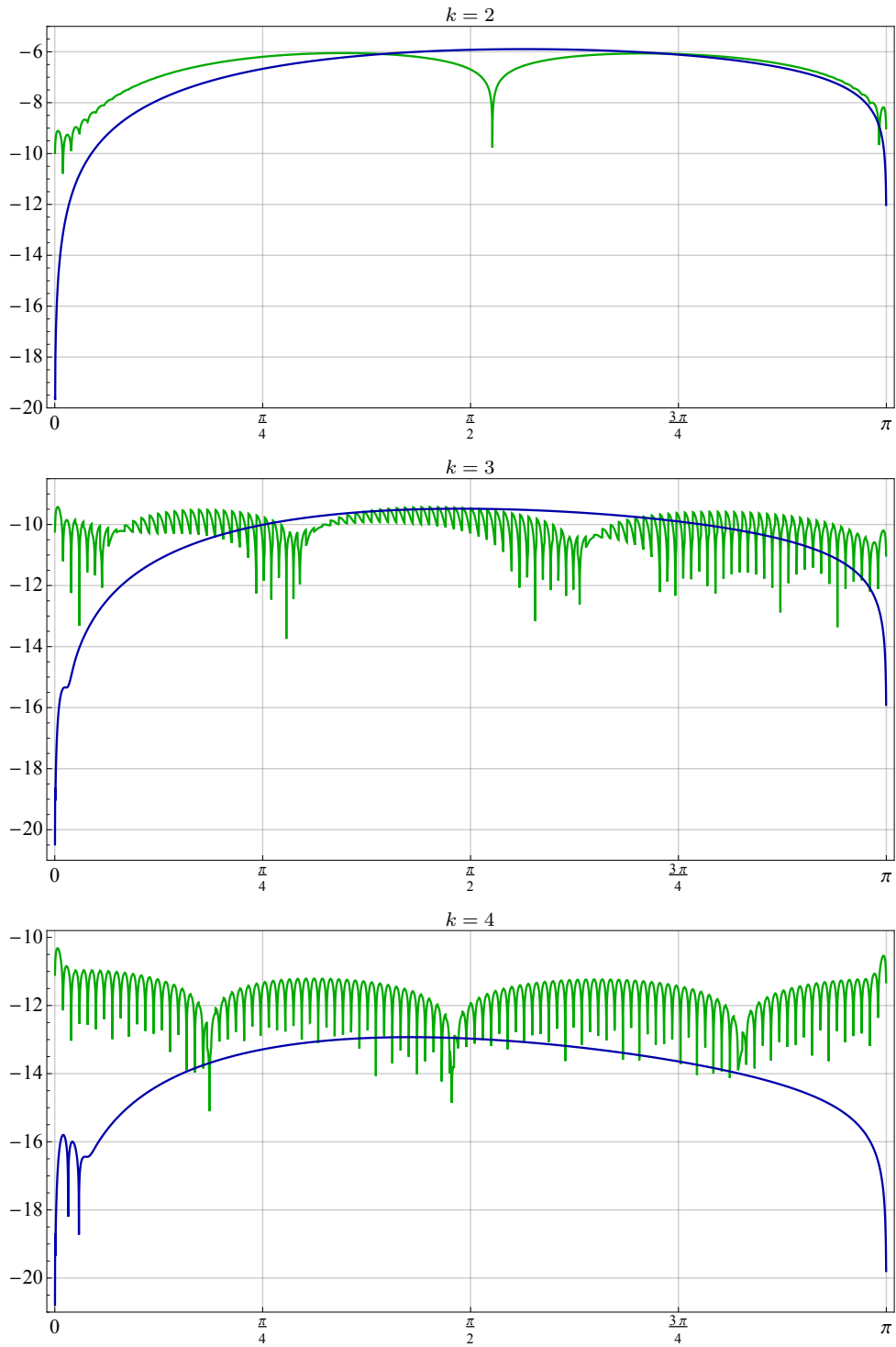


Figure 6: The same as Figure 5 but this time with $\ell = 3$.

Example 4.3 (A matrix order dependent symbol). We now test our algorithm with a symbol which is a linear combination of RCTPs with coefficients depending on the matrix order n . Consider the symbol

$$F_n(\theta) \equiv f_2(\theta) + \alpha_1 f_1(\theta)h^2 + \alpha_0 f_0(\theta)h^4, \quad (4.3)$$

where f_ℓ is given by (4.2) and α_ℓ are real constants. We previously studied this symbol in [8, §4.1] where we proposed an improvement to the numerical algorithm [14]. This symbol commonly arises when discretizing differential equations with the Finite Differences method.

The respective Fourier coefficients can be exactly calculated using the previous example and the linearity of the Fourier transform, as $\mathbf{a}_k(F_n) = \alpha_2 \mathbf{a}_k(f_2) + \alpha_1 \mathbf{a}_k(f_1)h^2 + \alpha_0 \mathbf{a}_k(f_0)h^4$. Therefore, the Toeplitz matrices $T_n(F_n)$ are banded and penta-diagonal. For implementing the numerical algorithm in [14], we need to assume an eigenvalue expansion with the form

$$\lambda_j(T_n(F_n)) = f_2(\theta_{j,n}) + \sum_{\ell=1}^{\alpha-1} c_\ell(\theta_{j,n})h^\ell + E_{\alpha,j,n},$$

where the coefficients c_ℓ are continuous and bounded functions from $[0, \pi]$ to \mathbb{R} , and the remainder (error) term $E_{\alpha,j,n}$ satisfies the inequality $|E_{\alpha,j,n}| \leq \kappa_\alpha h^\alpha$. For the respective boundary modification proposed in [8], we need to note that

$$\begin{aligned} c_2(0) = \alpha_1 f_1(0) = 0, & & c_2(\pi) = \alpha_1 f_1(\pi) = 4\alpha_1, \\ c_4(0) = \alpha_0 f_0(0) = 0, & & c_4(\pi) = \alpha_0 f_0(\pi) = \alpha_0, \end{aligned}$$

while $c_\ell(0) = c_\ell(\pi) = 0$ in any other case. The Figure 7 and the Table 4, show the data.

n	256	512	1024	2048	4096
$\varepsilon_{n,1}^{\text{MNA}}$	6.0007×10^{-3}	3.0088×10^{-3}	1.5065×10^{-3}	7.5377×10^{-4}	3.7702×10^{-4}
$\varepsilon_{n,1}^{\text{NAS}}$	6.0007×10^{-3}	3.0088×10^{-3}	1.5065×10^{-3}	7.5377×10^{-4}	3.7702×10^{-4}
$(n+1)\varepsilon_{n,1}^{\text{NAS}}$	1.5422×10^0	1.5435×10^0	1.5442×10^0	1.5445×10^0	1.5446×10^0
$\varepsilon_{n,2}^{\text{MNA}}$	3.9869×10^{-5}	1.0043×10^{-5}	2.5287×10^{-6}	6.3851×10^{-7}	1.6273×10^{-7}
$\varepsilon_{n,2}^{\text{NAS}}$	1.5208×10^{-5}	3.7944×10^{-6}	9.4766×10^{-7}	2.3679×10^{-7}	5.9184×10^{-8}
$(n+1)^2 \varepsilon_{n,2}^{\text{NAS}}$	1.0045×10^0	9.9858×10^{-1}	9.9563×10^{-1}	9.9416×10^{-1}	9.9342×10^{-1}
$\varepsilon_{n,3}^{\text{MNA}}$	9.2045×10^{-8}	1.0710×10^{-8}	3.6629×10^{-9}	1.8241×10^{-9}	9.1977×10^{-10}
$\varepsilon_{n,3}^{\text{NAS}}$	8.9731×10^{-8}	1.1313×10^{-8}	1.4203×10^{-9}	1.7792×10^{-10}	2.2264×10^{-11}
$(n+1)^3 \varepsilon_{n,3}^{\text{NAS}}$	1.5231×10^0	1.5274×10^0	1.5295×10^0	1.5306×10^0	1.5311×10^0
$\varepsilon_{n,4}^{\text{MNA}}$	3.4333×10^{-9}	2.1389×10^{-10}	5.3710×10^{-11}	2.5589×10^{-11}	1.2650×10^{-11}
$\varepsilon_{n,4}^{\text{NAS}}$	4.3281×10^{-9}	2.7008×10^{-10}	1.8110×10^{-11}	2.3324×10^{-12}	2.9853×10^{-13}
$(n+1)^4 \varepsilon_{n,4}^{\text{NAS}}$	1.8881×10^1	1.8705×10^1	1.9990×10^1	4.1112×10^1	8.4112×10^1

Table 4: The maximum errors $\varepsilon_{n,k}^{\text{MNA}}$, $\varepsilon_{n,k}^{\text{NAS}}$, and maximum normalized errors $(n+1)^k \varepsilon_{n,k}^{\text{NAS}}$ for the levels $k = 1, 2, 3, 4$ and different matrix sizes n , corresponding to the symbol (4.3) with $\alpha_0 = 3$ and $\alpha_1 = 2$. We used a grid of size $n_1 = 100$.

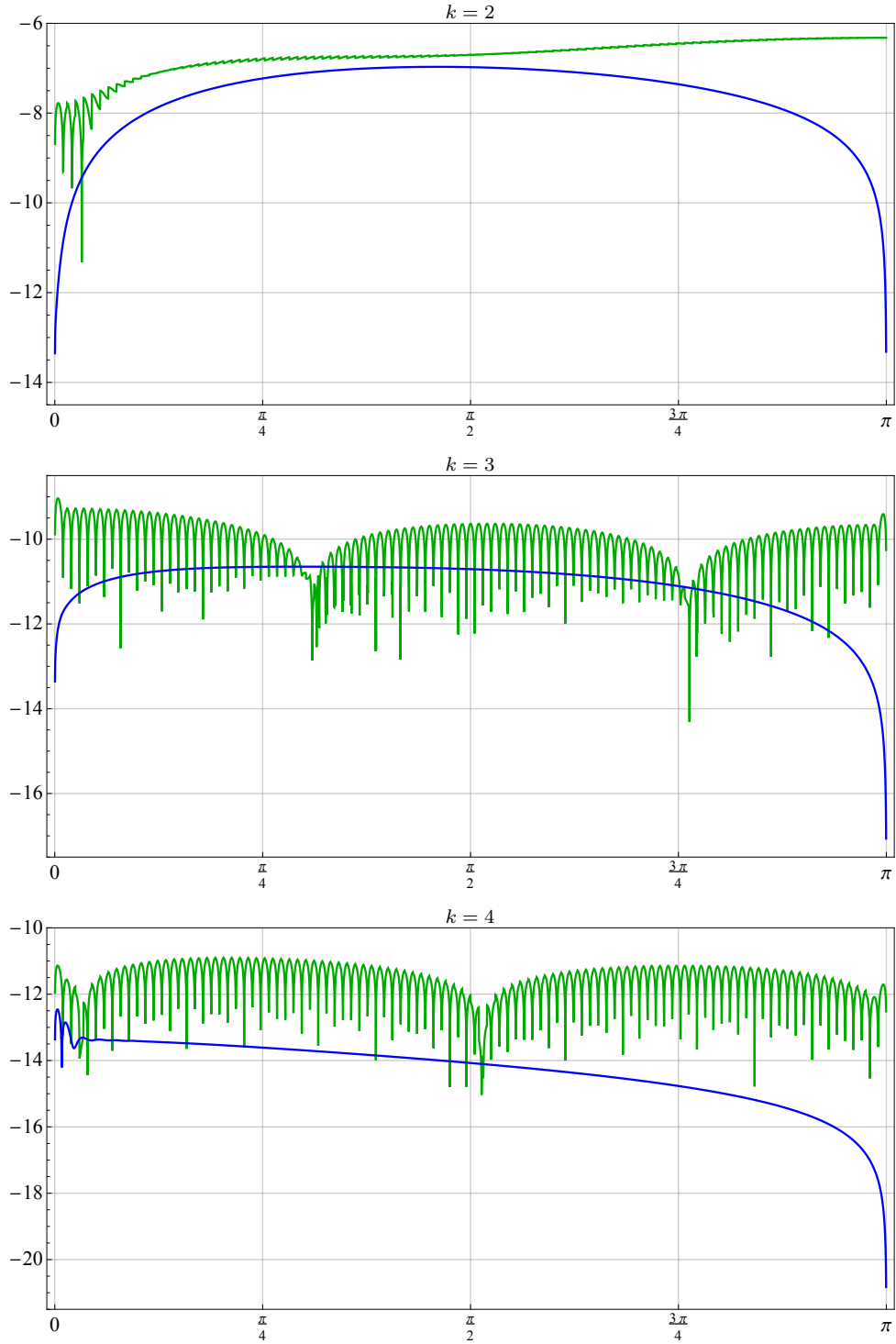


Figure 7: The base-10 logarithm for the individual errors $\varepsilon_{j,n,k}^{\text{SL}}$ (thick gray), $\varepsilon_{j,n,k}^{\text{MNA}}$ (green), and $\varepsilon_{j,n,k}^{\text{NAS}}$ (blue) for the matrix order dependent symbol F_n in (4.3), with $\alpha_0 = 3$, $\alpha_1 = 2$, a matrix size $n = 4096$, a grid size $n_1 = 100$, and different levels k .

5 CONCLUSIONS

Under appropriate technical assumptions, the simple-loop theory allows to deduce various types of asymptotic expansions for the eigenvalues of Toeplitz matrices $T_n(f)$ generated by a function f . Independently and under the milder hypothesis that f is even and monotonic over $[0, \pi]$, matrix-less algorithms have been developed for the fast eigenvalue computation of large Toeplitz matrices. These procedures work with a linear complexity in the matrix order n and behind the high efficiency of such algorithms there are the expansions predicted by the simple-loop theory, combined with the extrapolation idea.

In this note we have focused our attention on a change of variable, followed by the asymptotic expansion of the new variable that is

$$\lambda_j(T_n(f)) \equiv f(s_{j,n}), \quad s_{j,n} = \theta_{j,n} + \sum_{k=1}^{[\alpha]} r_k(\theta_{j,n})h^k + E_{j,n,\alpha},$$

and then we adapted the matrix-less to the considered new setting.

Numerical experiments have shown in a clear way a higher precision (till machine precision) and the same linear computation cost, when compared with the matrix-less procedures already presented in the relevant literature. More specifically, among the advantages, we concisely mention the following:

- a) when the coefficients of the simple-loop function are analytically known, the algorithm computes them perfectly;
- b) while the proposed algorithm is better or at worst comparable to the previous ones for the computation of the inner eigenvalues, it is extremely better for the computation of the extreme eigenvalues, which are essential for determining important quantities, like the conditioning in the positive definite case.

As next steps the following questions remain to be investigated:

- a fine error analysis for having a theoretical explanation of the reason why the new expansion leads to a much smaller errors, when compared with the numerical results in [12, 13, 15, 14];
- applications to the block cases (see [2, 3] for the theory in the block case) and related applications [12, 13] to differential problems;
- taking inspiration from [1], extension of the technique to preconditioned case $X_n = T_n^{-1}(g)T_n(l)$ in which g is positive over $(0, \pi)$ and is not identically constant, making use of the ergodic theorems given in [21], where Theorem 2.2 is extended to the preconditioned case in a very general setting.

REFERENCES

- [1] AHMAD, F., AL-AIDAROUS, E.S., ALREHAILI, D.A., EKSTRÖM, S.E., FURCI, I., AND SERRA-CAPIZZANO, S. Are the eigenvalues of preconditioned banded symmetric Toeplitz matrices known in almost closed form? *Numer. Algorithms* 78, 3 (2018), 867–893.

- [2] BARBARINO, G., GARONI, C., AND SERRA-CAPIZZANO, S. Block generalized locally Toeplitz sequences: Theory and applications in the multidimensional case. *Electron. Trans. Numer. Anal.* 53 (2020), 113–216.
- [3] BARBARINO, G., GARONI, C., AND SERRA-CAPIZZANO, S. Block generalized locally Toeplitz sequences: Theory and applications in the unidimensional case. *Electron. Trans. Numer. Anal.* 53 (2020), 28–112.
- [4] BARRERA, M., AND GRUDSKY, S.M. Asymptotics of eigenvalues for pentadiagonal symmetric Toeplitz matrices. *Oper. Theory: Adv. Appl.* 259 (2017), 51–77.
- [5] BOGOYA, M., BÖTTCHER, A., GRUDSKY, S.M., AND MAXIMENKO, E.A. Eigenvalues of Hermitian Toeplitz matrices with smooth simple-loop symbols. *Oper. Theory: Adv. Appl.* 422 (2015), 1308–1334.
- [6] BOGOYA, M., BÖTTCHER, A., GRUDSKY, S.M., AND MAXIMENKO, E.A. Eigenvectors of Hermitian Toeplitz matrices with smooth simple-loop symbols. *Linear Algebra Appl.* 493 (2016), 606–637.
- [7] BOGOYA, M., GRUDSKY, S.M., AND MAXIMENKO, E.A. Eigenvalues of Hermitian Toeplitz matrices generated by simple-loop symbols with relaxed smoothness. *Oper. Theory: Adv. Appl.* 259 (2017), 179–212.
- [8] BOGOYA, M., AND SERRA-CAPIZZANO, S. Eigenvalue superposition expansion for toeplitz matrix-sequences, generated by linear combinations of matrix-order dependent symbols, and applications to fast eigenvalue computations. *arXiv:2112.11794* (2022).
- [9] BÖTTCHER, A., BOGOYA, M., GRUDSKY, S.M., AND MAKSIMENKO, R. Asymptotics of the eigenvalues and eigenvectors of Toeplitz matrices. *Mat. Sb.* 208, 11 (2017), 4–28.
- [10] BÖTTCHER, A., AND SILBERMANN, B. *Introduction to large truncated Toeplitz matrices*. Universitext. Springer-Verlag, New York, 1999.
- [11] DAVIS, P.J. *Interpolation and approximation*. Dover, New York, 1975.
- [12] EKSTRÖM, S.E., FURCI, I., GARONI, C., MANNI, C., SERRA-CAPIZZANO, S., AND SPELEERS, H. Are the eigenvalues of the B-spline isogeometric analysis approximation of $-\delta u = \lambda u$ known in almost closed form? *Numer. Linear Algebra Appl.* 25, 5 (2018), e2198, 34 pp.
- [13] EKSTRÖM, S.E., FURCI, I., AND SERRA-CAPIZZANO, S. Exact formulae and matrix-less eigensolvers for block banded Toeplitz-like matrices. *BIT Numerical Mathematics* 58, 4 (2018), 937–968.
- [14] EKSTRÖM, S.E., AND GARONI, C. A matrix-less and parallel interpolation-extrapolation algorithm for computing the eigenvalues of preconditioned banded symmetric Toeplitz matrices. *Numer. Algor.* 80 (2019), 819–848.
- [15] EKSTRÖM, S.E., GARONI, C., AND SERRA-CAPIZZANO, S. Are the eigenvalues of banded symmetric Toeplitz matrices known in almost closed form? *Exper. Math.* 27, 4 (2018), 478–487.
- [16] GARONI, C., AND SERRA-CAPIZZANO, S. *Generalized Locally Toeplitz sequences: Theory and applications. Vol. I*. Springer, Cham, 2017.

- [17] GARONI, C., AND SERRA-CAPIZZANO, S. *Generalized Locally Toeplitz sequences: Theory and applications. Vol. II.* Springer, Cham, 2018.
- [18] GRENANDER, U., AND SZEGŐ, G. *Toeplitz forms and their applications*, second ed. California Monographs in Mathematical Sciences. Chelsea Publishing Co., New York, 1984.
- [19] KAC, M., MURDOCK, W.L., AND SZEGŐ, G. On the eigenvalues of certain Hermitian forms. *J. Rational Mech. Anal.* 2 (1953), 767–800.
- [20] SERRA-CAPIZZANO, S. The extension of the concept of the generating function to a class of preconditioned Toeplitz matrices. *Linear Algebra Appl.* 267 (1997), 139–161.
- [21] SERRA-CAPIZZANO, S. An ergodic theorem for classes of preconditioned matrices. *Linear Algebra Appl.* 282, 1-3 (1998), 161–183.
- [22] STOER, J., AND BULIRSCH, R. *Introduction to numerical analysis*, third ed. Springer, 2010.
- [23] TRENCH, W.F. Asymptotic distribution of the spectra of a class of generalized Kac–Murdock–Szegő matrices. *Linear Algebra Appl.* 294 (1999), 181–192.
- [24] TRENCH, W.F. *Spectral decomposition of Kac–Murdock–Szegő matrices.* The selected works of William F. Trench. http://works.bepress.com/william_trench/133, 2010.
- [25] TYRTYSHNIKOV, E.E., AND ZAMARASHKIN, N.L. Spectra of multilevel Toeplitz matrices: advanced theory via simple matrix relationships. *Linear Algebra Appl.* 270 (1998), 15–27.